Biogeosciences Discuss., 8, 10895–10933, 2011
www.biogeosciences-discuss.net/8/10895/2011/
doi:10.5194/bgd-8-10895-2011

Biogeosciences Discussions

Simulation of anthropogenic CO_2 uptake in the CCSM3.1 ocean circulation-biogeochemical model: comparison with data-based estimates

S. Wang[1,3], **J. K. Moore**[1], **F. W. Primeau**[1], **and S. Khatiwala**[2]

[1]Earth System Science, University of California, Irvine, CA 92697, USA
[2]Lamont Doherty Earth Observatory, Columbia University,Palisades, NY 10964, USA
[3]National Center for Atmospheric Research, Boulder, CO, 80307, USA

Received: 6 October 2011 – Accepted: 19 October 2011 – Published: 9 November 2011

Correspondence to: S. Wang (shanlinw@ucar.edu)

Published by Copernicus Publications on behalf of the European Geosciences Union.

Abstract

The global ocean has taken up a large fraction of the CO_2 released by human activities since the industrial revolution. Quantifying the oceanic anthropogenic carbon (C_{ant}) inventory and its variability is important for predicting the future global carbon cycle. The detailed comparison of data-based and model-based estimates is essential for the validation and continued improvement of our prediction capabilities. So far, three global estimates of oceanic C_{ant} inventory that are "data-based" and independent of global ocean circulation models have been produced: one based on the ΔC^* method, and two are based on reconstructions of the Green function for the surface-to-interior transport, the TTD method and the maximum entropy inversion method (KPH). The KPH method, in particular, is capable of reconstructing the history of C_{ant} inventory through the industrial era. In the present study we use forward model simulations of the Community Climate System Model (CCSM3.1) to estimate the C_{ant} inventory and compare the results with the data-based estimates. We also use the simulations to test several assumptions of the KPH method, including the assumption of constant climate and circulation, which is common to all the data-based estimates. Though the integrated estimates of global C_{ant} inventories are consistent with each other, the regional estimates show discrepancies up to 50 %. The CCSM3 model underestimates the total C_{ant} inventory, in part due to weak mixing and ventilation in the North Atlantic and Southern Ocean. Analyses of different simulation results suggest that key assumptions about ocean circulation and air-sea disequilibrium in the KPH method are generally valid on the global scale, but may introduce significant errors in C_{ant} estimates on regional scales. The KPH method should also be used with caution when predicting future oceanic anthropogenic carbon uptake.

1 Introduction

Since the industrial revolution, a large amount of carbon dioxide (CO_2) has been emitted into the atmosphere due to human activities. Increased atmospheric CO_2 is the

BGD
8, 10895–10933, 2011

largest contributor to the anthropogenic Greenhouse effect (Solomon et al., 2007). Given the importance of CO_2 to climate, it is crucial to understand the global carbon cycle. The ocean plays an important role in the global carbon cycle, modulating atmospheric CO_2 concentrations and climate. The global ocean has taken up 20 to 35 percent of CO_2 released by human activities since the industrial revolution (Houghton, 2007; Khatiwala et al., 2009; Sabine et al., 2004). Some studies have suggested that the oceanic carbon sink may have changed during the past few decades (Le Quéré et al., 2007; Lovenduski et al., 2007; Perez et al., 2010b; Wang and Moore, 2010; Wetzel et al., 2005), though significant uncertainties remain (e.g., McKinley et al., 2011). Quantifying the oceanic carbon inventory and its variability is therefore important for understanding the global carbon cycle and how it might change over time.

Anthropogenic carbon concentrations in the ocean cannot be measured directly and the magnitude of the anthropogenic carbon signal is only a few percent of the large natural background. Substantial effort has been made to estimate the oceanic anthropogenic CO_2 inventory and variability based on observational data and model simulations in recent years (Álvarez et al., 2009; Hall et al., 2004; Khatiwala et al., 2009; Mikaloff Fletcher et al., 2006; Sabine et al., 2004; Waugh et al., 2006). Generally, assessments of the oceanic CO_2 uptake based on observations can be made in two ways. One strategy is to estimate the uptake rates by repeated hydrographic measurements of the carbon system over time (e.g., Brown et al., 2010; Peng et al., 1998, 2003; Peng and Wanninkhof, 2010; Perez et al., 2010b; Murata et al., 2008, 2009; Sabine et al., 2008; Tanhua et al., 2007). However, interpreting the changes is complicated by the fact that the ocean carbon system exhibits significant natural variability on different timescales, from seasonal to decadal and longer timescales, and on different spatial scales. The variability complicates the investigation of oceanic anthropogenic carbon uptake rates and causes uncertainties in estimates of ocean carbon inventory.

The second strategy is to use back-calculation methods (eg. Gruber et al., 1996; Goyet et al., 1999; Tanhua et al., 2007; Touratier and Goyet, 2004; Touratier et al., 2007) and tracer-based calculations (eg. Hall et al., 2002; Waugh et al., 2006;

BGD
8, 10895–10933, 2011

Khatiwala et al., 2009) to estimate the anthropogenic carbon uptake. Since the estimates by Brewer (1978) and Chen and Millero (1979), several alternative methods have been developed to estimate the anthropogenic carbon inventory. One of the most widely used back-calculation methods is the ΔC^* method, which was developed by Gruber et al. (1996). The ΔC^* method starts with measured dissolved inorganic carbon (DIC) data. Biological and natural CO_2 solubility components of the DIC are removed with measured oxygen, nutrients, alkalinity and other observational data. The residual is interpreted as the anthropogenic signal. The first global estimate of C_{ant} inventory was carried out by applying this method to a subset of the Global Ocean Data Analysis Project (GLODAP) dataset (Sabine et al., 2004). The ΔC^* method is established based on several assumptions. First, the air-sea disequilibrium is constant. Second, the biological pump is constant and known. It also assumes constant ocean circulation with weak mixing. A previous study by Matsumoto and Gruber (2005) has evaluated uncertainties of the ΔC^* method with a global ocean biogeochemical model. Their results suggested that major biases arose from the assumption of constant disequilibrium and a single ventilation age.

A second approach is based on exploiting tracer observations (Hall et al., 2002). This method fully exploits the smallness of the anthropogenic perturbation to treat anthropogenic carbon as a passive, inert tracer. As a consequence, its concentration in the interior can be related to its time evolving history in the surface mixed layer via a Green function, the distribution of times needed for water to be transported from the surface to the interior (or transit time distribution (TTD)). This approach, known as the TTD method, assumes that biological productivity does not alter the uptake of anthropogenic carbon and that biological processes are not involved in the transport of tracers. The TTD method relaxes the assumption of a single ventilation time and avoids the need for uncertain biological corrections in the ΔC^* method. The along-isopycnal mixing of water masses of different ages is explicitly taken into account. Observational data are used to estimate the transit time distribution (i.e. the Green function) (Hall et al., 2002). The TTD method has been applied to assessments of oceanic anthropogenic carbon

BGD
8, 10895–10933, 2011

inventory (Hall et al., 2004; Waugh et al., 2004, 2006). Previous studies suggested that the assumptions of a single surface source region for water and anthropogenic CO_2, constant disequilibrium, the selection of a particular functional form for the Green function and the measurement limitation of transient tracers are probably the large sources of error in the TTD estimates (Hall et al., 2004; Waugh et al., 2006).

Recently, an alternative Green function method, has been developed by Khatiwala et al. (2009), which we refer to as the KPH method. This approach is also based on the notion of a TTD, but extends and improves in several aspects. The KPH method relaxes incorrect assumptions made in the ΔC^* method and/or the TTD method. The air-sea disequilibrium is allowed to evolve in space and time in the KPH method. The mixing of waters of both different ages and different end-member types is taken into account. An improved method of reconstructing the Green function using multiple steady and transient tracers made it possible to provide the first data-based estimate of the time-evolving, three-dimensional anthropogenic carbon distribution in the ocean starting at the beginning of the industrial revolution, unlike previous estimates which provided only a snapshot of the C_{ant} distribution. Another advantage of the KPH method is that it can, in principal, be used to predict the future anthropogenic carbon inventories in the ocean, given a projection of the future atmospheric CO_2 concentrations. The validity of such an estimate would however depend on the changes in the ocean's circulation and biological pump remaining negligibly small.

Previous observations suggest ongoing changes in the ocean. The heat content of the world ocean has increased substantially over the past few decades (Levitus et al., 2000, 2005) along with the global averaged sea surface temperature (Hansen et al., 2006, 2010). Changing temperatures can change both the uptake capacity for C_{ant} and the potential strength of the solubility pump (as reviewed by Friis, 2006). Dissolved oxygen concentrations have also decreased in several ocean basins (Andreev and Watanabe, 2002; Keller et al., 2002; Matear et al., 2000; Stramma et al., 2009). The ocean carbon pump and circulation may change in the future as the climate continues to change. Constant climate and ocean circulation is assumed in all the data-based

BGD
8, 10895–10933, 2011

estimates of anthropogenic carbon uptake. This assumption may introduce significant errors in studies of future anthropogenic carbon uptake, as suggested in previous research (Goodkin et al., 2011)

Coupled carbon cycle-ocean circulation models have also been used to estimate the ocean carbon inventory and assist the understanding of the global carbon cycle (e.g. Álvarez et al., 2009; Orr et al., 2001; Xu and Li, 2009). The strength of global carbon cycle models is that they can take into account the impact of changes in future climate. Carbon cycle models can also provide the opportunity to evaluate and interpret data-based estimates. However, given limited resolution and other model imperfections, carbon-cycle models do not necessarily agree with constraints provided by hydrographic tracer observations for the current era. It is necessary to evaluate the performance of carbon cycle models against data-based estimates of the anthropogenic carbon uptake. Several models have been evaluated in this way (Álvarez et al., 2009; Orr et al., 2001; Xu and Li, 2009). Discrepancies exist among different data-based estimates and uncertainties are caused by various assumptions. In a recent review, Sabine and Tanhua (2010) summarized advantages and disadvantages of several different data-based methods, including the TTD method and the ΔC^* method, but without a full assessment of each method. Some earlier data-based methods have been evaluated using carbon cycle model simulated data (Levine et al., 2008; Matsumoto and Gruber, 2005; Yool et al., 2010).

The first objective of this study is to evaluate the ability of a coupled carbon cycle-ocean circulation model to estimate oceanic anthropogenic carbon uptake and compare it with different data-based estimates of anthropogenic carbon inventory. Comparisons of the anthropogenic carbon inventory estimated using the KPH method and other global estimates from the ΔC^* method and the TTD method are included. Then, assumptions made in the KPH method are assessed with model simulations to determine the applicability of the assumptions made in the KPH method.

BGD
8, 10895–10933, 2011

2 Methods and model description

2.1 Coupled carbon cycle – ocean circulation model

The ocean circulation model used in this study is the coarse resolution, ocean circulation component of the National Center for Atmospheric Research (NCAR) Community Climate System Model 3.1 (CCSM3.1) (Collins et al., 2006; Yeager et al., 2006). The carbon cycle was simulated with an ocean biogeochemical/ecosystem model, the Biogeochemical Elemental Cycling (BEC) model (Moore et al., 2002, 2004). The model includes 25 vertical levels with 8 levels in the upper 103 m. It has 100 × 116 horizontal grid points. The longitudinal resolution is 3.6° and the latitudinal resolution varies in the range of 0.9°–2.0°, with finer resolution near the equator. The wind speed-mixing relation in the model was adjusted to better match the observed mixed layer depths in the Southern Ocean (de Boyer Montégut et al., 2004). This modification significantly reduces the model's mixed layer depth bias, from 18 m too shallow in the standard CCSM 3.1 model to a bias of 2 m too deep in the Southern Ocean (Wang and Moore, 2010).

The BEC model includes five phytoplankton functional groups, one zooplankton group and the biogeochemical cycling of multiple growth limiting nutrients (nitrate, ammonium, phosphate, iron and silicate) (Moore et al., 2004; Wang and Moore, 2010). The five phytoplankton groups were diatoms, diazotrophs, small phytoplankton, coccolithophores and *Phaeocystis* (Wang and Moore, 2010). The light-, nutrient-, and temperature-dependencies of phytoplankton growth rate are modeled multiplicatively. Phytoplankton growth rates decrease under nutrient stress according to Michaelis-Menten nutrient uptake kinetics. Phytoplankton photoadaptation is described by varying chlorophyll to nitrogen ratios based on the model of Geider et al. (1998). Ecosystem parameters were chosen based on field and laboratory data and were described in detail by Moore et al. (2002, 2004) and Wang and Moore (2010). The ecosystem module is coupled with an ocean biogeochemistry module, which includes full carbonate system thermodynamics and air-sea CO_2 and O_2 fluxes. The atmosphere component is

BGD
8, 10895–10933, 2011

not coupled in this study. Atmospheric conditions, including atmospheric CO_2 concentrations, are prescribed boundary conditions, so that there is no oceanic feedback to the atmosphere.

The model was spun up for 600 yr with repeating National Center for Environmental Prediction/National Center for Atmospheric Research (NCEP/NCAR) meteorological reanalysis climatology data and satellite-based estimates of climatological sea ice cover (Large and Yeager, 2004) to allow tracer fields in the model to approach an approximate steady state. The initial distributions of nutrients, inorganic carbon and alkalinity were based on the World Ocean Atlas (WOA) 2001 database (Conkright et al., 2002) and the GLODAP database (Key et al., 2004). Dissolved iron initialization was based on simulations from Moore and Braucher (2008). Dust deposition was the repeating annual climatology by Luo et al. (2003). Atmospheric CO_2 concentration was set to be 278 ppm for the model initialization. Model year 600 corresponds to year 1764.

Four simulations (summarized in Table 1) were conducted following the initial spin-up of 600 yr. The control simulation (Ctrl) was a continuation of the spin-up run, forced with the same repeating climatology data. Atmospheric CO_2 concentration remained fixed at 278 ppm. The control run represents the pre-industrial scenario. The second simulation (Cexp) was also forced with repeating climatology data, but the atmospheric CO_2 concentrations was prescribed according to the reconstructed historical record starting in 1765. In the third and fourth simulations, labeled Fexp and Texp, the coupled model was forced with a repeating climatological surface forcing until year 1947, at which point the NCEP/NCAR 6-hourly data for momentum, heat, and freshwater fluxes (Large and Yeager, 2009) were then used instead of the climatological boundary forcing. The Ice fraction satellite data were from the Scanning Multichannel Microwave Radiometer (SMMR) from 1978 to 1988 and Special Sensor Microwave/Imager after 1988 (Large and Yeager, 2004). For the period prior to 1978 where satellite ice fraction data were unavailable, we used climatological sea ice data. In Fexp, the atmospheric CO_2 concentration was kept fixed at 278 ppm, while in Texp we used the reconstructed

BGD
8, 10895–10933, 2011

atmospheric CO_2 concentrations for the years from 1765 onwards. Both Fexp and Texp represent scenarios where changing climate is taken into account. Model performance was previously evaluated against biogeochemical and physical observations (Wang and Moore, 2011).

2.2 Reviewing the assumptions made in the Green function (KPH) method

The KPH method is a generalization of the TTD method and is based on several key assumptions. First, the anthropogenic carbon perturbation is assumed to be a conservative tracer and its distribution in the ocean is only related to physical processes, i.e., the KPH method neglects possible changes in the biological pump. The KPH estimate of C_{ant} uptake makes use of a Green function, G, which is obtained by deconvolving hydrographic tracer data under a constant climate assumption. The Green function is then used to propagate the surface history of the anthropogenic carbon, C^s_{ant}, into the ocean interior.

In order to estimate the (unknown) surface history C^s_{ant} of anthropogenic carbon, the KPH method makes use of mass conservation, namely, the rate of change of inventory of C_{ant} is equal to the instantaneous air-sea flux of C_{ant}. The rate of change of inventory is given in terms of the convolution of the Green function with C^s_{ant}, while the flux is proportional to the change in surface disequilibrium of CO_2. The KPH method assumes that this change in air-sea disequilibrium ($\delta \Delta pCO_2$) at any given point is proportional to the anthropogenic CO_2 perturbation in the atmosphere, (δpCO_2^{atm}),

$$\delta \Delta pCO_2 \approx \varepsilon \times \delta pCO_2^{atm}, \quad (1)$$

where the proportionality constant, ε, is a function of space. This assumption, justified on the basis of simulations in a carbon cycle model, together with the CO_2 system equilibrium chemistry in seawater allows the known atmospheric CO_2 history to be related to the surface C^s_{ant} concentration. The unknown proportionality constant is then constrained by imposing mass conservation and requiring that the computed surface

BGD
8, 10895–10933, 2011

pCO_2 value for the year 2000 matches the observed value in the Takahashi database (Takahashi et al., 2009) (see Khatiwala et al., 2009, for details).

2.3 Estimates of the ΔC* method and the TTD method

Estimates of global anthropogenic carbon distributions by the ΔC^* method ($C_{ant\_\Delta C^*}$) and the TTD method (C_{ant_TTD}) were obtained from the GLODAP data website (http://cdiac.ornl.gov/oceans/glodap/GlopDV.html). Both anthropogenic CO_2 estimates were made on subsets of the GLODAP dataset (Key et al., 2004; Sabine et al., 2004; Waugh et al., 2006). The calculations using the ΔC^* method were made in different studies (Lee et al., 2003; Sabine et al., 1999, 2002) with slight differences in the detailed techniques and synthesized by Sabine et al. (2004, 2005). There are occurrences of negative values of anthropogenic carbon concentrations, mainly due to mapping errors and uncertainties in the dataset, which were set to zero by Sabine et al. (2004). These negative values are not physically possible, and are set to zero in comparisons of column inventories (Fig. 1) and total inventories (Table 2). In comparisons of regional anthropogenic carbon vertical distributions (Fig. 3), these negative values are kept to show the uncertainties in the method.

Global estimates by the TTD method were made by Waugh et al. (2006) with a pointwise version of this method applied to temperature, salinity and CFC-12 from the GLODAP dataset. The TTD method overestimated anthropogenic carbon concentrations in deep waters when CFC-12 is near or below the measurement detection limit of $\sim 0.005\,\mathrm{pmol\,kg^{-1}}$ (Waugh et al., 2006). This bias yields an anthropogenic carbon concentration of $2.5\,\mu\mathrm{mol\,kg^{-1}}$. In calculations of regional and global inventories estimated using the TTD method, all values of anthropogenic carbon concentrations less than $2.5\,\mu\mathrm{mol\,kg^{-1}}$ are set to zero (Waugh et al., 2006). Based on model evaluations of the TTD method, it was found that the TTD method overestimated the global anthropogenic carbon inventory by ~20 %, with the largest biases in the Southern Ocean. Waugh et al. (2006) corrected this positive bias by reducing the global anthropogenic carbon

BGD
8, 10895–10933, 2011

inventory by 20 %. The positive bias was not corrected in data comparisons in this study, since the non-uniform pattern of the bias make the correction difficult.

2.4 Definitions of anthropogenic carbon (C_{ant})

In data-based methods, the ocean circulation over the industrial period is generally assumed to be constant (although the KPH method allows for a seasonal cycle). Furthermore, while the KPH method allows a time-varying air-sea disequilibrium of CO_2, both the ΔC^* and TTD methods assume it to be constant. Given these assumptions, oceanic anthropogenic carbon should be defined as the uptake of emitted CO_2 by human activities, given the premise of approximately constant natural carbon system and constant climate. It is equivalent to the difference between DIC concentrations in the Cexp simulation and in the Ctrl simulation, i.e., $C_{ant\_cnst} = [DIC]_{Cexp} - [DIC]_{Ctrl}$.

Previous observational studies have suggested that there are long term trends in upper ocean temperatures in key oceanic water masses (as reviewed in the IPCC, 2007). These changes may have an impact on the carbon system in seawater. A better definition of oceanic anthropogenic carbon should include the effects of CO_2 induced climate change on C_{ant} uptake. This effect is neglected in the data-based methods, but can be estimated in coupled circulation-carbon cycle models. To calculate the anthropogenic carbon inventory based on this definition, the formula should be $C_{ant\_var} = [DIC]_{Texp} - [DIC]_{Fexp}$.

As suggested by Keeling (2005), the definition of the C_{ant} used in these data-based methods may be an incomplete measure of the change in the ocean carbon content, since the natural carbon system may also change under anthropogenic perturbations. There is another definition, which is transferred from the definition of atmospheric anthropogenic CO_2. The anthropogenic portion of CO_2 in the atmosphere is commonly known as the CO_2 concentration difference between modern time and pre-industrial era, i.e., the increased part of CO_2. This definition represents both gross CO_2 emissions by human activities and effects on atmospheric CO_2 due to changes in uptakes of CO_2 by land and ocean as a result of changing climate. A similar definition

BGD
8, 10895–10933, 2011

for the oceanic anthropogenic carbon is usually used in modeling studies (Le Quéré et al., 2010; Sarmiento et al., 1992; Tjiputra et al., 2010), which represents the oceanic uptake of increased atmospheric CO_2 and changes in the biological pump and the natural DIC storage due to changing climate. The formula used to calculate the complete C_{ant} is $C_{ant\_all} = [DIC]_{Texp} - [DIC]_{Ctrl}$. To evaluate the complete feedback between the ocean carbon system and climate, it is necessary to consider both changes in the natural carbon cycle and emitted anthropogenic CO_2.

3 Results and discussion

3.1 Oceanic anthropogenic carbon inventory

3.1.1 Global and regional inventories

Since estimates using the ΔC^* method and the TTD method are only available for 1994, we first compare the oceanic anthropogenic carbon inventories from the data based estimates and the model simulations for the year 1994. The global anthropogenic carbon inventory estimated using the ΔC^* method is 106 ± 17 Pg C (Sabine et al., 2004), while that from the TTD method was in the range of 94–121 Pg C. The TTD-based inventory has been corrected for a positive bias of ~ 20 % as per model-based evaluations (Waugh et al., 2006). The uncorrected C_{ant_TTD} is 134 Pg C, as shown in Fig. 1 and Table 2. The inventory estimated using the KPH method (C_{ant_KPH}) was 114 ± 22 Pg C (Khatiwala et al., 2009). These data-based estimates discussed in this study only include the open ocean, i.e., marginal seas and the Arctic Ocean are not included. The same mask is applied to the CCSM results to compare the same regions.

The simulated global inventory of anthropogenic carbon with the CCSM (C_{ant_cnst}) is 92 Pg C in the constant climate scenario (Cexp). This value falls roughly within the error bars of data-based estimates, but on the low end. It is about 20 % lower than the C_{ant_KPH} and about 14 % lower than the C_{ant_TTD} and the $C_{ant\_\Delta C^*}$. Despite the

BGD
8, 10895–10933, 2011

nominal agreement with the previously quoted error bars, we believe that the CCSM estimate is likely low for reasons to be discussed later on. The column inventories from data-based estimates and CCSM simulations showed a similar pattern, with high column inventories in the North Atlantic and the Southern Ocean (Fig. 1). The CCSM estimated C_{ant} under varying climate (Texp) is similar to that under constant climate (C_{ant_cnst}).

Regional inventories of anthropogenic carbon from different methods are shown in Table 2. The various estimates agree best in the Indian Ocean. The total C_{ant} in the Indian Ocean was ∼ 13 Pg C, with ∼ 2 Pg C in the North Indian Ocean and ∼ 11 Pg C in the South Indian Ocean (> −35° S). When the area south of 35° S is included, the values of C_{ant} were larger than 20 Pg C, which was greater than the estimate of C_{ant} in the Indian Ocean in the year 2000 by Hall and Primeau (2004) and Hall et al. (2004). Except the $C_{ant\_\Delta C^*}$, all other C_{ant} estimates in the deep South Indian Ocean reveal penetration of anthropogenic carbon, consistent with results by Álvarez et al. (2009). Estimates of C_{ant} in the Pacific Ocean were also consistent, in the range of 29 Pg C–35 Pg C with the lower bound set by C_{ant_cnst} and the upper bound set by C_{ant_TTD} (Table 2).

Estimated inventories of C_{ant} had less agreement in the Atlantic Ocean and the Southern Ocean. The C_{ant_TTD} in the Sothern Ocean was much larger than other estimates (Fig. 1 and Table 2). Model evaluations of the TTD method suggested that the TTD method overestimated the Cant inventory by 60 % in the Southern Ocean, due to a positive bias in the deep convection region primarily caused by the assumption of constant disequilibrium (Waugh et al., 2006). C_{ant} inventories estimated using the ΔC^* and KPH methods are the same in the North Atlantic Ocean, but the regional patterns of column inventories are different (Fig. 2). The column inventories of C_{ant_KPH} are higher in deep water formation region of the North Atlantic Ocean and lower in the low to mid-latitude region of the North Atlantic Ocean. These regional differences are averaged out over the entire North Atlantic Ocean. The estimated $C_{ant\_\Delta C^*}$ in the Southern Ocean was also significantly smaller than the C_{ant_KPH}, mainly because of the

BGD
8, 10895–10933, 2011

assumption of constant disequilibrium made in the ΔC^* method (Khatiwala et al., 2009). Previous model evaluation suggested that the ΔC^*-based estimate showed significant deviations from the "true" value in the high-latitude North Atlantic Ocean and the Southern Ocean and indicated that the estimate from this method may be erroneous in these regions (Levine et al., 2008). The estimated C_{ant} from the CCSM was smaller than estimates using data-based methods in both the Atlantic Ocean and the Southern Ocean (Table 2 and Fig. 2). Compared to the KPH method, the CCSM is 18 % and 33 % lower in the North Atlantic Ocean and the Southern Ocean, respectively. It is likely that the CCSM underestimated the C_{ant} in these two regions. The mixing in the CCSM is relatively weak at high latitudes, especially in the Southern Ocean. A previous study has suggested that the weak formation and ventilation of Antarctic Intermediate Water and mode waters in the Southern Ocean in the CCSM may cause a weak oceanic carbon sink (Thornton et al., 2009). If we include the Atlantic sector of the Southern Ocean, C_{ant} from the ΔC^* method, the KPH method, and from the CCSM are smaller than the estimate of Vázquez-Rodríguez et al. (2009), who suggested that the C_{ant} inventory in the South Atlantic Ocean was 22 ± 5 Pg C in 1994. Estimates for the North Atlantic Ocean cannot be compared directly with Vázquez-Rodríguez et al. (2009)'s study because of the different latitude ranges used in each estimate. However, the estimate for the North Atlantic Ocean using the TTD method was on the low end of all estimates in the study by Vázquez-Rodríguez et al. (2009), but nevertheless was the largest of all estimates we compared.

3.1.2 Vertical profiles of the estimated C_{ant}

As shown in Fig. 2 and Table 2, regional distributions of anthropogenic carbon estimated using different methods can be very different, though the total regional inventories are similar. Figure 3 shows vertical profiles of the regionally-averaged C_{ant} from data-based methods and the CCSM. The Southern Ocean is defined as areas south of 35° S. Regionally averaged C_{ant} vertical profiles estimated using different methods show similar patterns. The surface C_{ant} values are in the range of 44–56 mmol m^{-3} in

BGD
8, 10895–10933, 2011

most regions. The lowest surface C_{ant} value is in the Southern Ocean, in the range of 37–40 mmol m^{-3}. Though different C_{ant} inventory estimates show the largest difference in Southern Ocean (Table 2), estimated C_{ant} concentrations have the best agreement in the surface Southern Ocean (200 m). In most regions, C_{ant} values decrease rapidly with depth in upper ocean waters down to depths of 1000 m to 1500 m and remain approximately constant and low in deeper waters. The concentrations of C_{ant} in deep waters are highest in the North Atlantic Ocean, where there is strong deep convection and mixing. The upper-ocean C_{ant} (1000 ~ 1500 m) estimates from different methods fall in a wide range in most regions, especially in the Southern Hemisphere (Fig. 3).

The ΔC^*method produces negative values in deep waters in all the regions. This is probably due to technical errors and uncertainties of this method, but the cause is unclear (Sabine et al., 2005; Waugh et al., 2006). The negative values indicate certain issues in the ΔC^* method, which suggests clear problems in accuracies of the estimates of $C_{ant\_\Delta C^*}$. Values of the C_{ant_TTD} are highest in deep waters in most regions, especially in the Atlantic Ocean and the Southern Ocean. One major source of uncertainties in the TTD is the assumption of constant disequilibrium, used for estimating the surface C_{ant} history. A previous study showed that estimated C_{ant} in the TTD method overestimated the C_{ant} inventory by 5–10 % (Hall et al., 2004). Waugh et al. (2004) suggested that the estimated C_{ant} with constant disequilibrium assumption most likely represented the upper bounds of C_{ant}. Thus, high values of C_{ant_TTD} shown in Fig. 3 likely overestimate the C_{ant} inventory.

The C_{ant} estimated using the KPH method usually falls in the middle of the range of all estimated C_{ant} in these comparisons. The values of C_{ant_TTD} should be lower than the $C_{ant\_\Delta C^*}$, which assumes no mixing of waters (Hall et al., 2004; Olsen et al., 2010). The global C_{ant} inventory from the TTD method by Waugh et al. (2006) was under the assumption of constant disequilibrium in the industrial era. The estimate should be lowered if varying disequilibrium is allowed in calculations, especially in younger waters (Hall et al., 2004; Waugh et al., 2004). The KPH method, which is a generalization of the TTD method, is also based on the assumption that anthropogenic CO_2

BGD
8, 10895–10933, 2011

can be treated as a conservative tracer. But it relaxes some assumptions in the TTD method. The KPH method includes the mixing of waters with different ages and types and allows the disequilibrium to evolve through time. The allowance for an increasing air-sea disequilibrium explains why the C_{ant} inventory estimated using the KPH method is generally smaller than that from the TTD method. The differences in assumptions and considerations between the TTD method and the KPH method also explain why the C_{ant_TTD} need to be corrected for the positive bias, while the KPH method does not require such a correction.

The regionally-averaged C_{ant} estimated using the CCSM exhibits roughly similar vertical profiles with other estimated C_{ant}, but with some differences in the details. The C_{ant_cnst} from the CCSM falls on the upper end of all estimates in the upper 200 m in the Indian Ocean and the Pacific Ocean. There is a good agreement between the C_{ant_cnst} and the C_{ant_TTD} in the upper 200 m in the Atlantic Ocean, but both are $\sim 5\,mmol\,m^{-3}$ higher than the C_{ant_KPH}. The C_{ant} estimated using the CCSM turns out to be lower than other estimates of C_{ant} below 400 m. There are clear differences between the regional averaged C_{ant_cnst} and the C_{ant_all}, whereas the later one includes impacts of varying climate. The differences between the C_{ant_cnst} and the C_{ant_all} are in the range of $-4\,mmol\,m^{-3} \sim 6\,mmol\,m^{-3}$ in the upper 1000 m. The largest difference between the C_{ant_cnst} and other data-based C_{ant} are located along ventilation pathways, between 1000 m and 2500 m in the North Atlantic Ocean and between 500 m and 1500 m in the Southern Ocean. These differences are mainly due to weak mixing and ventilation in the Southern Ocean and the North Atlantic Ocean (Thornton et al., 2009). The weak downward transport of CO_2 in these two regions causes the CCSM to underestimate the global C_{ant} inventory. The differences between the modeled C_{ant} and the C_{ant_KPH} during 1948 to 2003 are also shown in Fig. 4. The global C_{ant} inventories estimated using the CCSM increase from $\sim 45\,Pg\,C$ to $\sim 107\,Pg\,C$ from 1948 to 2003, while the C_{ant_KPH} inventories increase from 57 Pg C to 132 Pg C. Through the study period, the C_{ant} estimated using the CCSM changes proportionally to the C_{ant_KPH}, a value about 80 % of the C_{ant_KPH}. The bias in circulation causes a bias in the uptake

BGD
8, 10895–10933, 2011

of anthropogenic carbon. The accumulation of this bias leads to increasing differences between the model simulated C_{ant} and the KPH estimate.

3.2 Assessment of assumptions of the KPH method

There are three major assumptions in the KPH method as reviewed in Sect. 2.2. With these assumptions, the KPH method can estimate the time-varying distribution of C_{ant} in the ocean, given tracer observations and the atmospheric CO_2 history. This provides an opportunity to understand the evolution of the oceanic C_{ant} inventory. The estimated uncertainties of the global C_{ant} inventory from the KPH method were around ± 20 %, which included uncertainties from tracer observations, gas-transfer coefficient, and the shape of the Green function (Khatiwala et al., 2009). Some possible uncertainties from assumptions of constant circulation, constant biological production, and a linear relationship between $\delta\Delta pCO_2$ and δpCO_2^{atm} in the KPH method, which has not been evaluated in previous studies, are assessed in this work.

Some previous research found increased CO_2 uptake by phytoplankton and seagrasses under higher CO_2 conditions (Palacios and Zimmerman, 2007; Riebesell et al., 2007). These results suggest that enriched CO_2 may stimulate ocean biological productivity and modify the cycling of nutrients, indicating possible biological effects on anthropogenic carbon uptake. Under such conditions, C_{ant} may not behave as a conservative tracer, although the strength of these effects is poorly constrained and likely smaller than the quoted uncertainty of the KPH method. It would be useful to evaluate such effects, but the BEC model does not include influences of changes in CO_2 concentrations on phytoplankton growth or calcification, i.e., the biology does not change with rising CO_2. The coupled BEC/CCSM is therefore not capable of testing the first assumption in the KPH method, because the same assumption is implicitly made in the BEC model. The other two assumptions can, however, be examined with the CCSM simulations. The KPH method is not applied to the coupled ocean carbon cycle model in this study as in previous assessments of the ΔC^* method by Matsumoto and Gruber (2005) and of the TTD method by Waugh et al. (2006). Instead, simulation results from

BGD
8, 10895–10933, 2011

different scenarios are analyzed and compared to determine the applicability of the assumptions made in the KPH method.

3.2.1 Assumption of constant circulation

The second assumption made by the KPH method is that ocean circulation is in a cyclostationary state, i.e., a seasonally repeating steady state. This assumption is made out of necessity, as there are insufficient observations available to constrain the Green function for a time-varying circulation. The KPH method therefore cannot capture the effect of climate change on ocean circulation and hence CO_2 uptake. To evaluate the potential errors, we compare changes in global C_{ant} inventories estimated using different CCSM simulations and the KPH method from 1948 to 2003 (Fig. 4).

As defined in Sect. 2.4, C_{ant_cnst} represents the oceanic anthropogenic carbon inventory under constant climate and constant circulation, while C_{ant_var} is the net increase in DIC due to rising atmospheric CO_2 if changing climate is taken into account. The difference between C_{ant_cnst} and C_{ant_var} is the difference in CO_2 uptake due to changing climate, and thus a measure of the error introduced due to the assumption of constant circulation in the KPH method. The globally integrated C_{ant_cnst} inventories and C_{ant_var} inventories match well in the period from 1948 to 2003 (Fig. 4). The difference between C_{ant_cnst} and C_{ant_var} is less than 1 % of the C_{ant} inventory estimate. To the extent that the variability in the CCSM circulation is representative of the true variability, our comparison implies that possible circulation changes due to climate change during the period of 1948 to 2003 have had little impact on the C_{ant} inventory. On a global scale, the assumption of constant circulation for the last few decades that is made in the KPH method and the other data-based estimates appears to be a reasonable one.

If the total anthropogenic perturbation on the ocean carbon system is considered, the anthropogenic carbon should be defined as C_{ant_all}, which includes changes in DIC storage due to both rising atmospheric CO_2 and changing climate. The difference between C_{ant_all} and C_{ant_cnst} is shown as $\Delta_{Texp-Cexp}$ in Fig. 4. $\Delta_{Texp-Cexp}$ values vary from -2 Pg C to 2 Pg C, which are greater than the difference between C_{ant_cnst} and

BGD
8, 10895–10933, 2011

C_{ant_var}. Overall difference between C_{ant_all} and C_{ant_cnst} are less than ±4 % of the total inventory, which is within the uncertainty of the KPH method (as well as other data-based techniques). Differences between C_{ant_all} and C_{ant_cnst} largely arise from changes in the natural carbon cycle, particularly from the solubility pump. (While the KPH method can take into account variations in sea surface temperature, salinity, and winds as it impacts the solubility pump, this was not done in their 2009 study.) The small impact of changing climate on both the natural carbon system and the uptake of C_{ant} suggests that the assumption of constant circulation and fixed Green functions are reasonable in the study period for the total anthropogenic perturbation estimate.

Values of $\Delta_{Texp-Cexp}$ are larger than 4 Pg C in the upper 500 m, and account for more than 10 % of the total anthropogenic carbon signal. Vertical profiles of C_{ant_all} and C_{ant_cnst} also show substantial differences in the upper ocean (Fig. 3). This suggests that the upper-ocean carbon cycle is sensitive to changes in physical fields caused by changing climate, but these differences tend to average out in the integrated carbon inventories. Climate change has had limited impacts on the natural carbon cycle. But it seems likely that both the solubility pump and the biological pump will be increasingly affected in future decades as climate continues to change. A modeling study suggested changes in the natural carbon content may be equivalent to a 5 % reduction in the C_{ant} inventory in 1994 (Matsumoto et al., 2010). Thus, the assumption of constant circulation may potentially cause a bias in predictions of the future ocean carbon inventory, although the magnitude of this bias is likely to be smaller than the uncertainty in the KPH and other data-based methods for C_{ant}.

3.2.2 Assumption about disequilibrium

The carbon system and CO_2 flux are calculated explicitly in the CCSM, as is the air-sea CO_2 disequilibrium (ΔpCO_2), which drives ocean uptake of anthropogenic carbon. To accurately estimate C_{ant} uptake from observations it is therefore necessary to have an estimate of the space- and time-varying disequilibrium. To address this problem, Khatiwala et al. (2009) assumed that the change in disequilibrium ($\delta\Delta pCO_2$) is proportional

BGD
8, 10895–10933, 2011

to the anthropogenic perturbation on the atmospheric CO_2 (δpCO_2^{atm}). This assumption of a linear relationship between $\delta\Delta pCO_2$ and δpCO_2^{atm} was justified on the basis of simulations in an ocean carbon cycle model which showed a similar relationship (Fig. S1 by Khatiwala et al., 2009). By combining this relationship with surface ocean pCO_2 measurements and nonlinear CO_2 system chemistry, the KPH method can arrive at an estimate of the surface ocean time history of anthropogenic carbon. Here, we assess this assumption with our CCSM simulations, focusing in particular on the effect of climate change. The $\delta\Delta pCO_2$ is calculated using differences of ΔpCO_2 between two simulations with reconstructed CO_2 concentrations and the pre-industrial CO_2 concentration, respectively. Changes in the disequilibrium ($\delta\Delta pCO_{2\_var}$) for C_{ant} uptake under changing climate are calculated as the difference between ΔpCO_2 in Texp and Fexp. Similarly, in the case including both changes in the natural carbon system and the C_{ant} uptake, $\delta\Delta pCO_{2\_all}$ is the difference between ΔpCO_2 in Texp and Ctrl. The δpCO_2^{atm} is calculated based on the historical atmospheric CO_2 records used in the simulations. An approximate linear relationship can be found in simulations under constant climate (Ctrl and Cexp). However, there is a much weaker linear relationship between $\delta\Delta pCO_2$ and δpCO_2^{atm} in the cases that include the effects of changing climate (not shown). There are significant interannual and decadal variations in $\delta\Delta pCO_2$, which do not follow changes in atmospheric CO_2 very closely. These variations are mainly due to the effects of varying climate on the natural carbon system and/or the biological pump.

Figure 5 shows the standard errors (SSE) in the linear relationship between $\delta\Delta pCO_{2\_var}$ and δpCO_2^{atm} and between $\delta\Delta pCO_{2\_all}$ and δpCO_2^{atm}, where ε in the linear relationship of $\delta\Delta pCO_2 = \varepsilon \times \delta pCO_2^{atm}$ is determined using ordinary least squares with data from year 1765 to year 2003. Therefore the errors shown in Fig. 5 are the minimum that could be achieved given the linear relationship assumption. The magnitude of errors in the assumption of linear relationship between $\delta\Delta pCO_{2\_var}$ and δpCO_2^{atm} are usually 10 % ~ 25 % of the averaged $\delta\Delta pCO_{2\_var}$. The SSE is generally small in regions where changes in the disequilibrium are small. The errors are larger in

BGD
8, 10895–10933, 2011

the Arctic Ocean, the North Atlantic Ocean, the Equatorial Pacific and the Southern Ocean. The deviations from the assumed linear relationship in the Arctic Ocean are likely due to the presence of sea ice that inhibits the CO_2 exchange. The magnitude of SSE in this region is generally 10 % ~ 30 % of the $\delta\Delta pCO_2$. However, the Arctic Ocean is not included in the KPH estimate. There is a significant cancellation of errors when the $\delta\Delta pCO_{2\_var}$ is averaged over a 10-yr period, but on shorter time scales substantial errors remain. The SSE is larger than 50 % of the averaged $\delta\Delta pCO_{2\_all}$ in most of the ocean and more than 100 % in many areas. The errors are also larger in the Arctic Ocean, the North Atlantic Ocean, and increased significantly in the Equatorial Pacific and areas along the Antarctic continental shelf. These errors are mainly due to variations of the natural carbon system under changing climate. The values of SSE are still larger than 2 ppm in many areas after the $\delta\Delta pCO_{2\_all}$ is smoothed over 10 yr. It indicates that the bias caused by this assumption of the linear relationship may need to be considered, if the total anthropogenic perturbation in the ocean carbon system (equivalent to the C_{ant_all}) is considered. Calculating the history of CO_2 flux using the linear relationship may cause significant biases on regional scales, especially in large-SSE regions such as the southernmost Southern Ocean, the North Atlantic Ocean, the Equatorial Pacific Ocean, and areas with high biological productivity. However, it is likely those errors are smoothed out when averaging over large spatial scales (as done in the KPH method). It is also possible that positive and negative errors in C_{ant} induced by errors in the assumed linear relationship compensate each other when integrated globally, as indicated by the small differences between C_{ant_cnst}, C_{ant_var} and C_{ant_all} (Fig. 4).

Based on analyses of different simulations from 1948 and 2003, the assumptions of constant circulation and linear relationship between $\delta\Delta pCO_2$ and δpCO_2^{atm} in the KPH method are acceptable for estimates on the global scale during this period, especially on longer time scales. In the cases, when complete anthropogenic perturbation is considered, the assumption of constant circulation and linear relationship is likely to cause ± 2 Pg C uncertainties to the estimate (this can be compared to the roughly

BGD
8, 10895–10933, 2011

± 20 Pg C uncertainty in the 2008 estimate of C_{ant} based on the KPH method). One needs to pay close attention to uncertainties in the assumption. Previous studies suggested that the CO_2 flux and the spatial patterns of pCO_2 distributions linked closely to variability in the climate forcing (Doney et al., 2009; Feely et al., 2006; Le Quéré et al., 2010; Park et al., 2010; Takahashi et al., 2003; Thomas et al., 2008; Ullman et al., 2009). Some recent research on decadal trends suggests that the efficiency of the ocean to absorb CO_2 has decreased in the Southern Ocean and North Atlantic Ocean (Corbière et al., 2007; Metzl, 2009; Sabine and Gruber, 2006; Schuster and Watson, 2007), though others suggest smaller trends in carbon sink based on data on longer timescale and larger spatial scales (McKinley et al., 2011). The uncertainties associated with these assumptions may increase, especially on regional scales, if the ongoing climate change continues to perturb the natural carbon cycle.

4 Summary

In this study, three widely used data-based global estimates of oceanic anthropogenic carbon inventories were compared with the C_{ant} inventories simulated using BEC/CCSM coupled model under different forcing scenarios. The largest differences among C_{ant} estimates occur in the Southern Ocean. Though the integrated C_{ant} inventories are similar in the North Atlantic Ocean, this is the region of second largest spatial discrepancies between the estimates. The differences in these regions are mainly due to the different assumptions made in each method. The oceanic anthropogenic carbon estimated using different data-based methods show quite different spatial patterns, though the globally integrated C_{ant} inventories are consistent. The coupled model can generally reproduce the oceanic anthropogenic carbon inventory and distribution patterns, but it is likely to underestimate the global C_{ant} inventory. The modeled global inventory of anthropogenic carbon is 92 Pg C in simulations with constant climate and the estimates are similar in simulations with changing climate. The model estimates are roughly within the error bars of data-based estimates, but on the low end of the

BGD
8, 10895–10933, 2011

range. The CCSM mainly underestimates the C_{ant} inventory in the Southern Ocean and the North Atlantic Ocean. This is primarily due to weak deep mixing and ventilation in those regions. To better estimate and predict C_{ant} inventories, priority should be given to improving the ocean circulation component of the CCSM. Though the C_{ant} inventories of C_{ant_all} and C_{ant_cnst} are similar after being integrated, the spatial patterns are different due to impacts of different climate forcing.

The differences between the estimates from the ΔC^* method and the TTD method have been examined in previous studies (Hall et al., 2002; Waugh et al., 2006). Both estimates were significantly biased due to the assumption of constant disequilibrium. The KPH method allows the disequilibrium to evolve through time and includes the mixing of waters of different types, and is therefore likely to produce more realistic estimates of C_{ant}. Overall, the comparisons of vertical and regional distributions of the C_{ant} estimates show that the KPH method has more advanced skills in estimating the C_{ant} inventory and distributions and its estimate of the C_{ant} inventory seems reliable for investigating the global C_{ant} inventory in the past and for constraining ocean carbon models.

Our simulations suggest that the assumption of constant ocean circulation during the last few decades made by all the data-based estimates is reasonable. There is less than 1 % difference between estimates of the C_{ant} inventories under constant climate (constant circulation) and varying climate. If changes in the natural cycle system caused by varying climate are taken into account, the uncertainty due to this assumption is less than 4 % of the C_{ant} inventory, which falls within the uncertainty of data-based estimates. The accuracy of calculations of the carbon history in the surface ocean is closely related to the linear-relationship assumption. Our analysis suggests that the linear relationship between changes in air-sea disequilibrium and changes in atmospheric CO_2 is a good approximation under constant climate. There are substantial errors in the assumption of linear relationship in simulations with changing climate, especially if the complete anthropogenic perturbation on the ocean carbon system is considered. While these errors may cause significant biases in estimates on regional

BGD
8, 10895–10933, 2011

scales and interannual time scales, they largely average out on large spatial scales and on time scales of decades or longer. The KPH method depends critically on the assumption that changes in the ocean circulation do not affect the uptake of anthropogenic CO_2. Uncertainties in its regional estimates may be larger, especially for the Southern Ocean, North Atlantic and Equatorial Pacific. Recent research on decadal trends shows that the capacity of the ocean to uptake CO_2 may have decreased in these regions (Corbière et al., 2007; Metzl, 2009; Sabine and Gruber, 2006; Schuster and Watson, 2007), where the linear relationship assumption may be problematic. The KPH method should be used with caution in predicting future oceanic anthropogenic carbon uptake, with careful consideration of uncertainties due to changing climate.

In this study, we have also tried to clarify the definition of anthropogenic carbon in the ocean. For the purpose of closing the carbon budget of the atmosphere, the land and the ocean, the anthropogenic carbon should be defined as the ocean uptake of increased atmospheric CO_2 under changing climate. A more broad and complete definition of the anthropogenic perturbation on the ocean carbon system should include the uptake of anthropogenic CO_2 and changes in the natural carbon system. Some studies have showed that changes in the natural carbon cycle contributed to observed changes in the DIC, and that transport and distributions of anthropogenic CO_2 may be affected by climate variability (Thomas et al., 2008; Wanninkhof et al., 2010). With the knowledge that the global ocean has been undergoing many changes (Hansen et al., 2010; Levitus et al., 2005; Thompson and Solomon, 2002), the broader definition of anthropogenic carbon perturbation should be adopted in global carbon cycle research. So far, model-based assessments have shown that many data-based methods have substantial potential errors (Levine et al., 2008; Matsumoto and Gruber, 2005; Waugh et al., 2006; Yool et al., 2010). It seems that what is needed is reduction and better quantification of errors on regional scales in data-based methods so that model errors can be better pinned down. It is also necessary to further develop the data-based methods and models and to characterize related uncertainties based on sustained observations in order to understand the variability of the ocean carbon system.

BGD
8, 10895–10933, 2011

Acknowledgements. This work was supported by funding from NASA grants NNG05GR25G and NNX08AB76G to J. K. Moore, and NSF grant OCE 07-27229 to S. Khatiwala. Computations were supported by the Earth System Modeling Facility at University of California, Irvine (NSF ATM-O321380). Thanks to I. Lima and K. Lindsay for support in model simulations used in this study.

References

Álvarez, M., Lo Monaco, C., Tanhua, T., Yool, A., Oschlies, A., Bullister, J. L., Goyet, C., Metzl, N., Touratier, F., McDonagh, E., and Bryden, H. L.: Estimating the storage of anthropogenic carbon in the subtropical Indian Ocean: a comparison of five different approaches, Biogeosciences, 6, 681–703, doi:10.5194/bg-6-681-2009, 2009.

Andreev, A. and Watanabe, S.: Temporal changes in dissolved oxygen of the intermediate water in the Subarctic North Pacific, Geophys. Res. Lett., 29, 1680, doi:10.1029/2002gl015021, 2002.

de Boyer Montégut, C., Madec, G., Fischer, A. S., Lazar, A., and Iudicone, D.: Mixed layer depth over the global ocean: an examination of profile data and a profile-based climatology, J. Geophys. Res., 109, C12003, doi:10.1029/2004jc002378, 2004.

Brewer, P. G.: Direct observation of the oceanic CO_2 increase, Geophys. Res. Lett., 5, 997–1000, 1978.

Brown, P. J., Bakker, D. C. E., Schuster, U., and Watson, A. J.: Anthropogenic carbon accumulation in the Subtropical North Atlantic, J. Geophys. Res.-Oceans, 115, C04016, doi:10.1029/2008jc005043, 2010.

Chen, G.-T. and Millero, F. J.: Gradual increase of oceanic CO_2, Nature, 277, 205–206, 1979.

Collins, W. D., Bitz, C. M., Blackmon, M. L., Bonan, G. B., Bretherton, C. S., Carton, J. A., Chang, P., Doney, S. C., Hack, J. J., Henderson, T. B., Kiehl, J. T., Large, W. G., McKenna, D. S., Santer, B. D., and Smith, R. D.: The Community Climate System Model version 3 (CCSM3), J. Climate, 19, 2122–2143, doi:10.1175/JCLI3761.1, 2006.

Conkright, M. E., Locarnini, R. A., Garcia, H. E., O'Brien, T. D., Boyer, T. P., Stephens, C., and Antonov, J. J.: World Ocean Atlas 2001: Objective analysis, data statistics, and figures, CDROM documentation, National Oceanographic Data Center, Silver Spring, MD, 2002.

Corbière, A., Metzl, N., Reverdin, G., Brunet, C., and Takahashi, T.: Interannual and decadal variability of the oceanic carbon sink in the North Atlantic subpolar gyre, Tellus B, 59, 168–178, doi:10.1111/j.1600-0889.2006.00232.x, 2007.

BGD

8, 10895–10933, 2011

Doney, S. C., Lima, I., Feely, R. A., Glover, D. M., Lindsay, K., Mahowald, N., Moore, J. K., and Wanninkhof, R.: Mechanisms governing interannual variability in upper-ocean inorganic carbon system and air-sea CO_2 fluxes: physical climate and atmospheric dust, Deep-Sea Res. Pt. II, 56, 640–655, doi:10.1016/j.dsr2.2008.12.006, 2009.

Feely, R. A., Takahashi, T., Wanninkhof, R., McPhaden, M. J., Cosca, C. E., Sutherland, S. C., and Carr, M.-E.: Decadal variability of the air-sea CO_2 fluxes in the Equatorial Pacific Ocean, J. Geophys. Res., 111, C08S90, doi:10.1029/2005jc003129, 2006.

Friis, K.: A review of marine anthropogenic CO_2 definitions: introducing a thermodynamic approach based on observations, Tellus B, 58, 2–15, doi:10.1111/j.1600-0889.2005.00173.x, 2006.

Geider, R. J., MacIntyre, H. L., and Kana, T. M.: A dynamic regulatory model of phytoplanktonic acclimation to light, nutrients, and temperature, Limnol. Oceanogr., 43, 679–694, 1998.

Goodkin, N. F., Levine, N. M., Doney, S. C., and Wanninkhof, R.: Impacts of temporal CO_2 and climate trends on the detection of ocean anthropogenic CO_2 accumulation, Global Biogeochem. Cy., 25, GB3023, doi:10.1029/2010gb004009, 2011.

Goyet, C., Coatanoan, C., Eischeid, G., Amaoka, T., Okuda, K., Healy, R., and Tsunogai, S.: Spatial variation of total CO_2 and total alkalinity in the Northern Indian Ocean: a novel approach for the quantification of anthropogenic CO_2 in seawater, J. Mar. Res., 57, 135–163, 1999.

Gruber, N., Sarmiento, J. L., and Stocker, T. F.: An improved method for detecting anthropogenic CO_2 in the oceans, Global Biogeochem. Cy., 10, 809–837, doi:10.1029/96gb01608, 1996.

Hall, T. M. and Primeau, F. W.: Separating the natural and anthropogenic air-sea flux of CO_2: the Indian Ocean, Geophys. Res. Lett., 31, L23302, doi:10.1029/2004gl020589, 2004.

Hall, T. M., Haine, T. W. N., and Waugh, D. W.: Inferring the concentration of anthropogenic carbon in the ocean from tracers, Global Biogeochem. Cy., 16, 1131, doi:10.1029/2001gb001835, 2002.

Hall, T. M., Waugh, D. W., Haine, T. W. N., Robbins, P. E., and Khatiwala, S.: Estimates of anthropogenic carbon in the Indian Ocean with allowance for mixing and time-varying air-sea CO_2 disequilibrium, Global Biogeochem. Cy., 18, GB1031, doi:10.1029/2003gb002120, 2004.

Hansen, J., Sato, M., Ruedy, R., Lo, K., Lea, D. W., and Medina-Elizade, M.: Global temperature change, P. Natl. Acad. Sci. USA, 103, 14288–14293, doi:10.1073/pnas.0606291103, 2006.

BGD
8, 10895–10933, 2011

Hansen, J., Ruedy, R., Sato, M., and Lo, K.: Global surface temperature change, Rev. Geophys., 48, RG4004, doi:10.1029/2010rg000345, 2010.
Houghton, R. A.: Balancing the global carbon budget, Annu. Rev. Earth Pl. Sc., 35, 313–347, doi:10.1146/annurev.earth.35.031306.140057, 2007.
Keeling, R. F.: Comment on "The Ocean Sink for Anthropogenic CO_2", Science, 308, 1743, doi:10.1126/science.1109620, 2005.
Keller, K., Slater, R. D., Bender, M., and Key, R. M.: Possible biological or physical explanations for decadal scale trends in North Pacific nutrient concentrations and oxygen utilization, Deep-Sea Res. Pt. II, 49, 345–362, doi:10.1016/s0967-0645(01)00106-0, 2002.
Key, R. M., Kozyr, A., Sabine, C. L., Lee, K., Wanninkhof, R., Bullister, J. L., Feely, R. A., Millero, F. J., Mordy, C., and Peng, T. H.: A global ocean carbon climatology: results from Global Data Analysis Project (GLODAP), Global Biogeochem. Cy., 18, GB4031, doi:10.1029/2004gb002247, 2004.
Khatiwala, S., Primeau, F., and Hall, T.: Reconstruction of the history of anthropogenic CO_2 concentrations in the ocean, Nature, 462, 346–349, doi:10.1038/nature08526, 2009.
Large, W. G. and Yeager, S. G.: Diurnal to decadal global forcing for ocean and sea-ice models: the data sets and flux climatologies, NCAR Technical Note NCAR/TN-460+STR., 2004.
Large, W. G. and Yeager, S. G.: The global climatology of an interannually varying air–sea flux data set, Clim. Dynam., 33, 341–364, doi:10.1007/s00382-008-0441-3, 2009.
Le Quéré, C., Rodenbeck, C., Buitenhuis, E. T., Conway, T. J., Langenfelds, R., Gomez, A., Labuschagne, C., Ramonet, M., Nakazawa, T., Metzl, N., Gillett, N., and Heimann, M.: Saturation of the Southern Ocean CO_2 sink due to recent climate change, Science, 316, 1735–1738, doi:10.1126/science.1136188, 2007.
Le Quéré, C., Takahashi, T., Buitenhuis, E. T., Rodenbeck, C., and Sutherland, S. C.: Impact of climate change and variability on the global oceanic sink of CO_2, Global Biogeochem. Cy., 24, GB 4007, doi:10.1029/2009gb003599, 2010.
Lee, K., Choi, S. D., Park, G. H., Wanninkhof, R., Peng, T. H., Key, R. M., Sabine, C. L., Feely, R. A., Bullister, J. L., Millero, F. J., and Kozyr, A.: An updated anthropogenic CO_2 inventory in the Atlantic Ocean, Global Biogeochem. Cy., 17, 1116, doi:10.1029/2003gb002067, 2003.
Levine, N. M., Doney, S. C., Wanninkhof, R., Lindsay, K., and Fung, I. Y.: Impact of ocean carbon system variability on the detection of temporal increases in anthropogenic CO_2, J. Geophys. Res., 113, C03019, doi:10.1029/2007jc004153, 2008.

BGD
8, 10895–10933, 2011

Levitus, S., Antonov, J. I., Boyer, T. P., and Stephens, C.: Warming of the world ocean, Science, 287, 2225–2229, doi:10.1126/science.287.5461.2225, 2000.
Levitus, S., Antonov, J., and Boyer, T.: Warming of the world ocean, 1955–2003, Geophys. Res. Lett., 32, L02604, doi:10.1029/2004gl021592, 2005.
Lovenduski, N. S., Gruber, N., Doney, S. C., and Lima, I. D.: Enhanced CO_2 outgassing in the Southern Ocean from a positive phase of the Southern Annular Mode, Global Biogeochem. Cy., 21, GB2026, doi:10.1029/2006gb002900, 2007.
Luo, C., Mahowald, N. M., and del Corral, J.: Sensitivity study of meteorological parameters on mineral aerosol mobilization, transport, and distribution, J. Geophys. Res., 108, 4447, doi:10.1029/2003jd003483, 2003.
Matear, R. J., Hirst, A. C., and McNeil, B. I.: Changes in dissolved oxygen in the Southern Ocean with climate change, Geochem. Geophys. Geosy., 1, 1050 pp., doi:10.1029/2000gc000086, 2000.
Matsumoto, K. and Gruber, N.: How accurate is the estimation of anthropogenic carbon in the ocean? An evaluation of the Delta C* method, Global Biogeochem. Cy., 19, GB3014, doi:10.1029/2004gb002397, 2005.
Matsumoto, K., Tokos, K. S., Chikamoto, M. O., and Ridgwell, A.: Characterizing post-industrial changes in the ocean carbon cycle in an Earth system model, Tellus B, 62, 296–313, doi:10.1111/j.1600-0889.2010.00461.x, 2010.
McKinley, G. A., Fay, A. R., Takahashi, T., and Metzl, N.: Convergence of atmospheric and North Atlantic carbon dioxide trends on multidecadal timescales, Nature Geoscience, 4, 606–610, doi:10.1038/ngeo1193, 2011.
Metzl, N.: Decadal increase of oceanic carbon dioxide in Southern Indian Ocean surface waters (1991–2007), Deep-Sea Res. Pt. II, 56, 607–619, doi:10.1016/j.dsr2.2008.12.007, 2009.
Mikaloff Fletcher, S. E., Gruber, N., Jacobson, A. R., Doney, S. C., Dutkiewicz, S., Gerber, M., Follows, M., Joos, F., Lindsay, K., Menemenlis, D., Mouchet, A., Müller, S. A., and Sarmiento, J. L.: Inverse estimates of anthropogenic CO_2 uptake, transport, and storage by the ocean, Global Biogeochem. Cy., 20, GB2002, doi:10.1029/2005gb002530, 2006.
Moore, J. K. and Braucher, O.: Sedimentary and mineral dust sources of dissolved iron to the world ocean, Biogeosciences, 5, 631–656, doi:10.5194/bg-5-631-2008, 2008.
Moore, J. K., Doney, S. C., Kleypas, J. A., Glover, D. M., and Fung, I. Y.: An intermediate complexity marine ecosystem model for the global domain, Deep-Sea Res. Pt. II, 49, 403–462, doi:10.1016/S0967-0645(01)00108-4, 2002.

BGD
8, 10895–10933, 2011

Moore, J. K., Doney, S. C., and Lindsay, K.: Upper ocean ecosystem dynamics and iron cycling in a global three-dimensional model, Global Biogeochem. Cy., 18, GB4028, doi:10.1029/2004gb002220, 2004.

Murata, A., Kumamoto, Y., Sasaki, K., Watanabe, S., and Fukasawa, M.: Decadal increases of anthropogenic CO_2 in the Subtropical South Atlantic Ocean along 30° S, J. Geophys. Res.-Oceans, 113, C06007, doi:10.1029/2007jc004424, 2008.

Murata, A., Kumamoto, Y., Sasaki, K. I., Watanabe, S., and Fukasawa, M.: Decadal increases of anthropogenic CO_2 along 149° E in the Western North Pacific, J. Geophys. Res.-Oceans, 114, C04018, 04012, doi:10.1029/2008jc004920, 2009.

Olsen, A., Omar, A. M., Jeansson, E., Anderson, L. G., and Bellerby, R. G. J.: Nordic seas transit time distributions and anthropogenic CO_2, J. Geophys. Res., 115, C05005, doi:10.1029/2009jc005488, 2010.

Orr, J. C., Maier-Reimer, E., Mikolajewicz, U., Monfray, P., Sarmiento, J. L., Toggweiler, J. R., Taylor, N. K., Palmer, J., Gruber, N., Sabine, C. L., Le Quéré, C., Key, R. M., and Boutin, J.: Estimates of anthropogenic carbon uptake from four three-dimensional global ocean models, Global Biogeochem. Cy., 15, 43–60, doi:10.1029/2000gb001273, 2001.

Palacios, S. L. and Zimmerman, R. C.: Response of eelgrass Zostera marina to CO_2 enrichment: possible impacts of climate change and potential for remediation of coastal habitats, Mar. Ecol.-Prog. Ser., 344, 1–13, doi:10.3354/meps07084, 2007.

Park, G.-H., Wanninkhof, R. I. K., Doney, S. C., Takahashi, T., Lee, K., Feely, R. A., Sabine, C. L., TriÑanes, J., and Lima, I. D.: Variability of global net sea–air CO_2 fluxes over the last three decades using empirical relationships, Tellus B, 62, 352–368, doi:10.1111/j.1600-0889.2010.00498.x, 2010.

Peng, T.-H. and Wanninkhof, R.: Increase in anthropogenic CO_2 in the Atlantic Ocean in the last two decades, Deep-Sea Res. Pt. I, 57, 755–770, doi:10.1016/j.dsr.2010.03.008, 2010.

Peng, T.-H., Wanninkhof, R., Bullister, J. L., Feely, R. A., and Takahashi, T.: Quantification of decadal anthropogenic CO_2 uptake in the ocean based on dissolved inorganic carbon measurements, Nature, 396, 560–563, doi:10.1038/25103, 1998.

Peng, T.-H., Wanninkhof, R., and Feely, R. A.: Increase of anthropogenic CO_2 in the Pacific Ocean over the last two decades, Deep-Sea Res. Pt. II, 50, 3065–3082, doi:10.1016/j.dsr2.2003.09.001, 2003.

Pérez, F. F., Aristegui, J., Vazquez-Rodriguez, M., and Rios, A. F.: Anthropogenic CO_2 in the Azores region, Sci. Mar., 74, 11–19, doi:10.3989/scimar.2010.74s1011, 2010a.

BGD

8, 10895–10933, 2011

Pérez, F. F., Vázquez-Rodríguez, M., Mercier, H., Velo, A., Lherminier, P., and Ríos, A. F.: Trends of anthropogenic CO_2 storage in North Atlantic water masses, Biogeosciences, 7, 1789–1807, doi:10.5194/bg-7-1789-2010, 2010b.

Riebesell, U., Schulz, K. G., Bellerby, R. G. J., Botros, M., Fritsche, P., Meyerhofer, M., Neill, C., Nondal, G., Oschlies, A., Wohlers, J., and Zollner, E.: Enhanced biological carbon consumption in a high CO_2 ocean, Nature, 450, 545–548, doi:10.1038/nature06267, 2007.

Sabine, C. L. and Gruber, N.: Introduction to special section on North Pacific Carbon Cycle Variability and Climate Change, J. Geophys. Res., 111, C07S01, doi:10.1029/2006jc003532, 2006.

Sabine, C. L. and Tanhua, T.: Estimation of anthropogenic CO_2 inventories in the ocean, Ann. Rev. Mar. Sci., 2, 175–198, doi:10.1146/annurev-marine-120308-080947, 2010.

Sabine, C. L., Key, R. M., Johnson, K. M., Millero, F. J., Poisson, A., Sarmiento, J. L., Wallace, D. W. R., and Winn, C. D.: Anthropogenic CO_2 inventory of the Indian Ocean, Global Biogeochem. Cy., 13, 179–198, doi:10.1029/1998gb900022, 1999.

Sabine, C. L., Key, R. M., Bullister, J. L., Millero, F. J., Lee, K., Peng, T. H., Tilbrook, B., Ono, T., and Wong, C. S.: Distribution of anthropogenic CO_2 in the Pacific Ocean, Global Biogeochem. Cy., 16, 1083, doi:10.1029/2001gb001639, 2002.

Sabine, C. L., Feely, R. A., Gruber, N., Key, R. M., Lee, K., Bullister, J. L., Wanninkhof, R., Wong, C. S., Wallace, D. W. R., Tilbrook, B., Millero, F. J., Peng, T.-H., Kozyr, A., Ono, T., and Rios, A. F.: The oceanic sink for anthropogenic CO_2, Science, 305, 367–371, doi:10.1126/science.1097403, 2004.

Sabine, C. L., Key, R. M., Kozyr, A., Feely, R. A., Wanninkhof, R., Millero, F. J., Peng, T.-H., Bullister, J. L., and Lee, K.: Global Ocean Data Analysis Project: Results and Data, ORNL/CDIAC-145, NDP-083. Carbon Dioxide Information Analysis Center, Oak Ridge National Laboratory, US Department of Energy, Oak Ridge, Tennessee, 110 pp., 2005.

Sabine, C. L., Feely, R. A., Millero, F. J., Dickson, A. G., Langdon, C., Mecking, S., and Greeley, D.: Decadal changes in Pacific carbon, J. Geophys. Res.-Oceans, 113, C07021, doi:10.1029/2007jc004577, 2008.

Sarmiento, J. L., Orr, J. C., and Siegenthaler, U.: A perturbation simulation of CO_2 uptake in an ocean general circulation model, J. Geophys. Res., 97, 3621–3645, doi:10.1029/91jc02849, 1992.

Schuster, U. and Watson, A. J.: A variable and decreasing sink for atmospheric CO_2 in the North Atlantic, J. Geophys. Res., 112, C11006, doi:10.1029/2006jc003941, 2007.

BGD
8, 10895–10933, 2011

Solomon, S., Qin, D., Manning, M., Chen, Z., Marquis, M., Averyt, K. B., Tignor, M., and Miller, H. L.: IPCC Fourth Assessment Report: Climate Change 2007, Cambridge University Press, Cambridge, United Kingdom and New York, NY, USA., 2007.

Stramma, L., Visbeck, M., Brandt, P., Tanhua, T., and Wallace, D.: Deoxygenation in the oxygen minimum zone of the Eastern Tropical North Atlantic, Geophys. Res. Lett., 36, L20607, doi:10.1029/2009GL039593, 2009.

Takahashi, T., Sutherland, S. C., Feely, R. A., and Cosca, C. E.: Decadal variation of the surface water pCO_2 in the Western and Central Equatorial Pacific, Science, 302, 852–856, doi:10.1126/science.1088570, 2003.

Takahashi, T., Sutherland, S. C., Wanninkhof, R., Sweeney, C., Feely, R. A., Chipman, D. W., Hales, B., Friederich, G., Chavez, F., Sabine, C., Watson, A., Bakker, D. C. E., Schuster, U., Metzl, N., Yoshikawa-Inoue, H., Ishii, M., Midorikawa, T., Nojiri, Y., Körtzinger, A., Steinhoff, T., Hoppema, M., Olafsson, J., Arnarson, T. S., Tilbrook, B., Johannessen, T., Olsen, A., Bellerby, R., Wong, C. S., Delille, B., Bates, N. R., and de Baar, H. J. W.: Climatological mean and decadal change in surface ocean pCO_2, and net sea-air CO_2 flux over the global oceans, Deep-Sea Res. Pt. II, 56, 554–577, doi:10.1016/j.dsr2.2008.12.009, 2009.

Tanhua, T., Kortzinger, A., Friis, K., Waugh, D. W., and Wallace, D. W. R.: An estimate of anthropogenic CO_2 inventory from decadal changes in oceanic carbon content, P. Natl. Acad. Sci. USA, 104, 3037–3042, doi:10.1073/pnas.0606574104, 2007.

Thomas, H., Prowe, A. E. F., Lima, I. D., Doney, S. C., Wanninkhof, R., Greatbatch, R. J., Schuster, U., and Corbiere, A.: Changes in the North Atlantic oscillation influence CO_2 uptake in the North Atlantic over the past 2 decades, Global Biogeochem. Cy., 22, GB4027, doi:10.1029/2007gb003167, 2008.

Thompson, D. W. J. and Solomon, S.: Interpretation of recent Southern Hemisphere climate change, Science, 296, 895–899, doi:10.1126/science.1069270, 2002.

Thornton, P. E., Doney, S. C., Lindsay, K., Moore, J. K., Mahowald, N., Randerson, J. T., Fung, I., Lamarque, J.-F., Feddema, J. J., and Lee, Y.-H.: Carbon-nitrogen interactions regulate climate-carbon cycle feedbacks: results from an atmosphere-ocean general circulation model, Biogeosciences, 6, 2099–2120, doi:10.5194/bg-6-2099-2009, 2009.

Tjiputra, J. F., Assmann, K., and Heinze, C.: Anthropogenic carbon dynamics in the changing ocean, Ocean Sci., 6, 605–614, doi:10.5194/os-6-605-2010, 2010.

Touratier, F. and Goyet, C.: Definition, properties, and Atlantic Ocean distribution of the new tracer TrOCA, J. Mar. Sys., 46, 169–179, doi:10.1016/j.jmarsys.2003.11.016, 2004.

BGD

8, 10895–10933, 2011

Touratier, F., Azouzi, L., and Goyet, C.: CFC-11, Δ14C and 3H tracers as a means to assess anthropogenic CO_2 concentrations in the ocean, Tellus B, 59, 318–325, doi:10.1111/j.1600-0889.2006.00247.x, 2007.

Ullman, D. J., McKinley, G. A., Bennington, V., and Dutkiewicz, S.: Trends in the North Atlantic carbon sink: 1992–2006, Global Biogeochem. Cy., 23, GB4011, doi:10.1029/2008gb003383, 2009.

Vázquez-Rodríguez, M., Touratier, F., Lo Monaco, C., Waugh, D. W., Padin, X. A., Bellerby, R. G. J., Goyet, C., Metzl, N., Ríos, A. F., and Pérez, F. F.: Anthropogenic carbon distributions in the Atlantic Ocean: data-based estimates from the Arctic to the Antarctic, Biogeosciences, 6, 439–451, doi:10.5194/bg-6-439-2009, 2009.

Wang, S. and Moore, J. K.: Variability of primary production and air-sea CO_2 flux in the Southern Ocean, Global Biogeochem. Cy., submitted, 2010.

Wang, S. and Moore, J. K.: Incorporating *Phaeocystis* into a Southern Ocean ecosystem model, J. Geophys. Res., 116, C01019, doi:10.1029/2009jc005817, 2011.

Wanninkhof, R., Doney, S. C., Bullister, J. L., Levine, N. M., Warner, M., and Gruber, N.: Detecting anthropogenic CO_2 changes in the Interior Atlantic Ocean between 1989 and 2005, J. Geophys. Res.-Oceans, 115, C11028, doi:10.1029/2010jc006251, 2010.

Waugh, D. W., Haine, T. W. N., and Hall, T. M.: Transport times and anthropogenic carbon in the Subpolar North Atlantic Ocean, Deep-Sea Res. Pt. I, 51, 1475–1491, doi:10.1016/j.dsr.2004.06.011, 2004.

Waugh, D. W., Hall, T. M., McNeil, B. I., Key, R., and Matear, R. J.: Anthropogenic CO_2 in the oceans estimated using transit time distributions, Tellus B, 58, 376–389, doi:10.1111/j.1600-0889.2006.00222.x, 2006.

Wetzel, P., Winguth, A., and Maier-Reimer, E.: Sea-to-air CO_2 flux from 1948 to 2003: a model study, Global Biogeochem. Cy., 19, GB2005, doi:10.1029/2004gb002339, 2005.

Xu, Y. and Li, Y.: Estimates of anthropogenic CO_2 uptake in a global ocean model, Adv. Atmos. Sci., 26, 265–274, doi:10.1007/s00376-009-0265-z, 2009.

Yeager, S. G., Shields, C. A., Large, W. G., and Hack, J. J.: The low-resolution CCSM3, J. Climate, 19, 2545–2566, doi:10.1175/JCLI3744.1, 2006.

Yool, A., Oschlies, A., Nurser, A. J. G., and Gruber, N.: A model-based assessment of the TrOCA approach for estimating anthropogenic carbon in the ocean, Biogeosciences, 7, 723–751, doi:10.5194/bg-7-723-2010, 2010.

BGD
8, 10895–10933, 2011

Table 1. Simulation descriptions.

Simulation	AtmCO_2	Forcing	Description
Ctrl	278 ppm	constant climate	provides information of oceanic DIC distributions under the pre-industrial scenario
Cexp	ramp up after 1765	constant climate	provides information of anthropogenic carbon storage in the ocean under constant climate
Fexp	278 ppm	varying climate after 1948	provides information of changes in natural oceanic carbon system under the changing climate
Texp	ramp up after 1765	varying climate after 1948	represents the combined effects of rising atmospheric CO_2 and the changing climate on oceanic carbon storage

BGD
8, 10895–10933, 2011

Table 2. Regional and global distributions of C_{ant} inventories in 1994 (in PgC).

Region	ΔC^* method	TTD method	KPH method	CCSM(C_{ant_cnst})	CCSM(C_{ant_all})
N. Pacific	16	17	18	18	17
S. Pacific	13	18	16	15	15
N. Indian	3	2	2	2	2
S. Indian	11	11	11	10	10
N. Atlantic	22	24	22	18	18
S. Atlantic	10	11	8	6	6
Southern Ocean[a]	30	49	36	22	23
Global	106	133[b]	114	92	93

[a] The Southern Ocean is defined as south of 35° S.
[b] The value calculated by Waugh et al. (2006) is 134 Pg C. The difference may occur due to rounding error.

BGD
8, 10895–10933, 2011

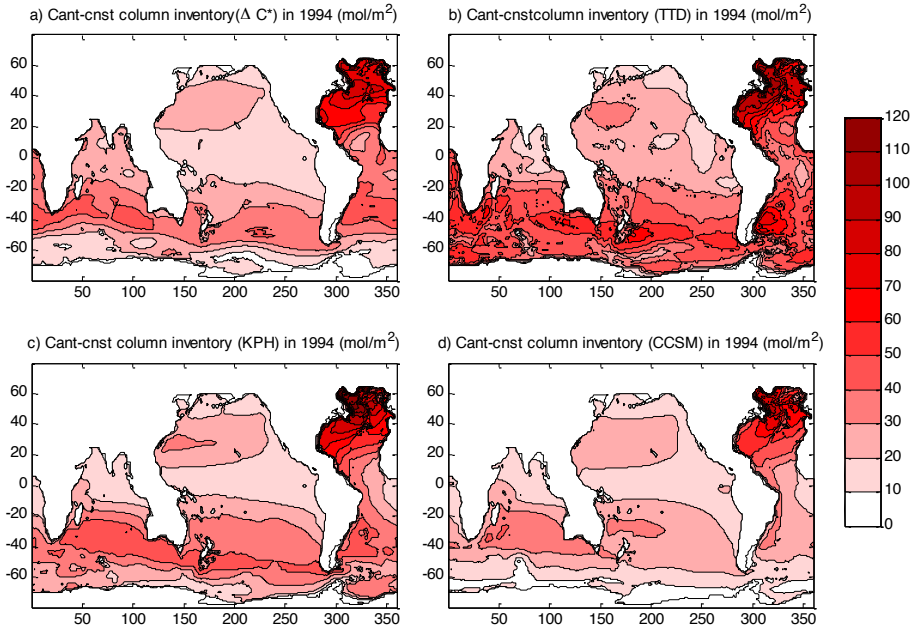

Fig. 1. Column inventories of anthropogenic DIC in year 1994 by **(a)** the ΔC^* method; **(b)** the TTD method; **(c)** the KPH method; **(d)** the CCSM (C_{ant_cnst}).

BGD
8, 10895–10933, 2011

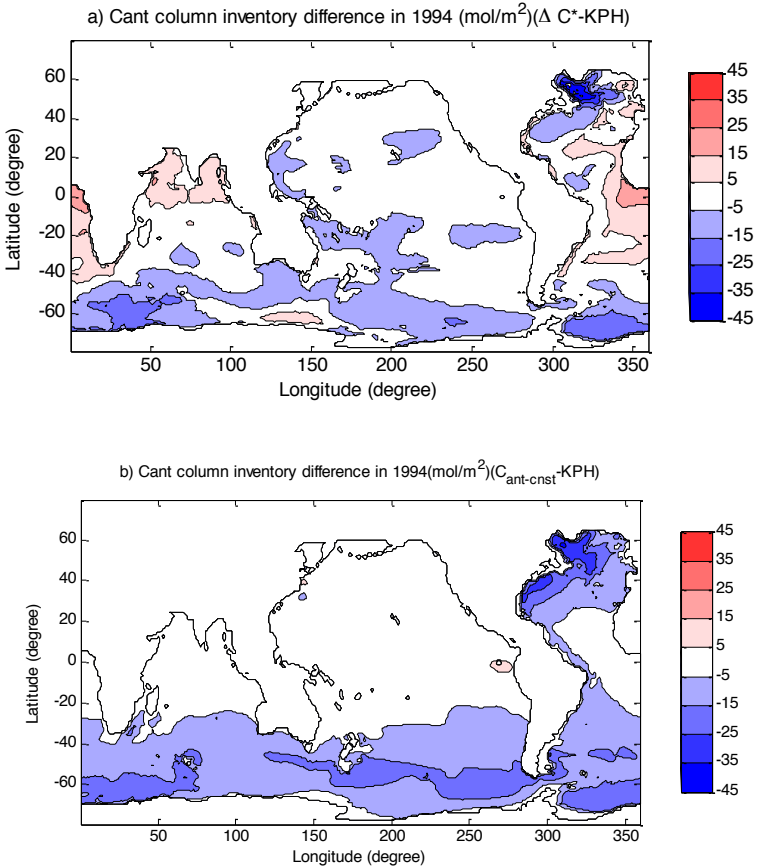

Fig. 2. Differences in column inventories between **(a)** the ΔC^* method and the KPH method; **(b)** the CCSM (C_{ant_cnst}) and the KPH method.

BGD
8, 10895–10933, 2011

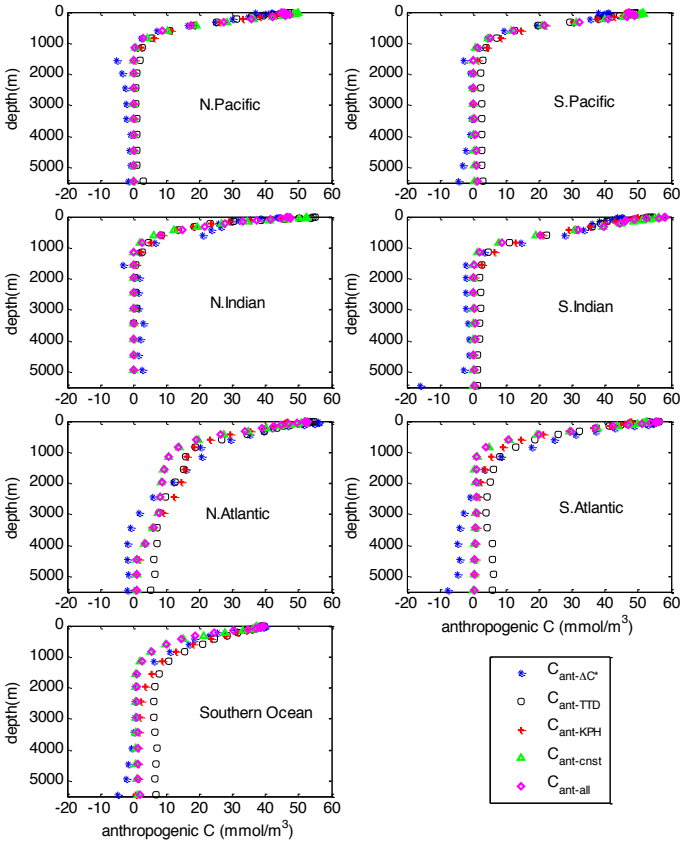

Fig. 3. Comparison of regional averaged C_{ant} from the ΔC^* method (blue asterisk), the TTD method (black circle), the KPH method (red cross), the C_{ant_cnst} from the CCSM (green triangle), and the C_{ant_all} from the CCSM (magenta diamond). The Southern Ocean is south of 35° S. Data were vertically interpolated to compare values at the same depth.

BGD
8, 10895–10933, 2011

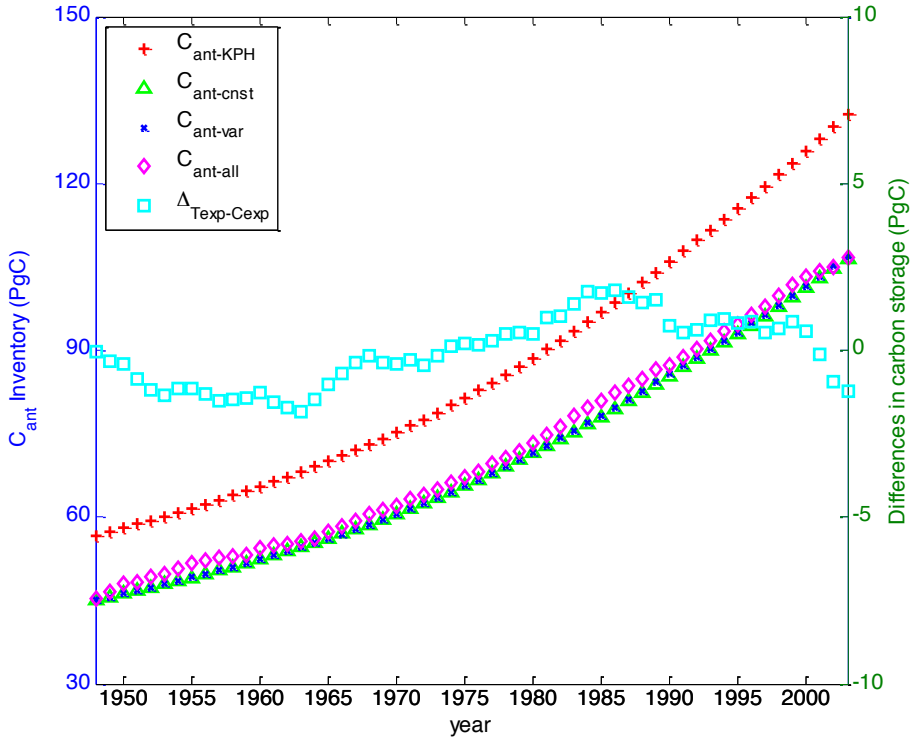

Fig. 4. Changes in the estimated ocean C_{ant} inventories, estimated using the KPH method and the CCSM, through time (the left axis) and the differences in total DIC inventory from two simulations forced with rising atmospheric CO_2 (the right axis). Shown are: C_{ant_KPH} (red crosses); C_{ant_cnst} (green triangles); C_{ant_var} (blue crosses); C_{ant_all} (magenta diamonds). The cyan squares show the differences between total DIC in the Texp and in the Cexp. $\Delta_{Texp-Cexp} = C_{ant\_all} - C_{ant\_cnst}$.

BGD
8, 10895–10933, 2011

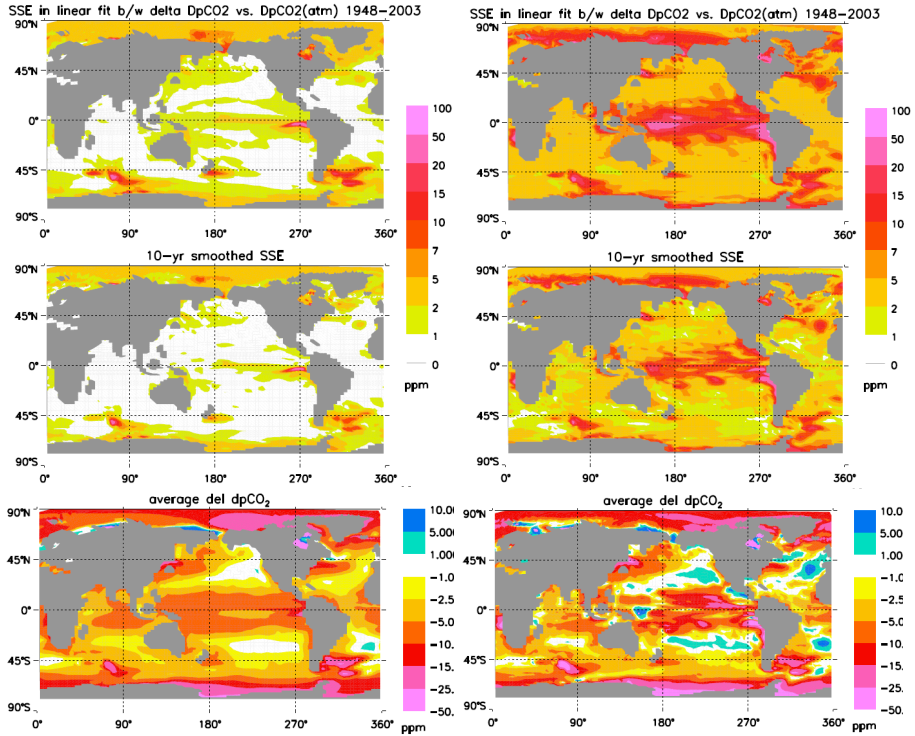

Fig. 5. Maps of the standard error (top two panels) in the linear relationship between $\delta\Delta pCO_2$ and δpCO_2^{atm} with varying climate on annual time scale; maps of 10-yr smoothed standard errors (middle two panels); and maps of mean $\delta\Delta pCO_2$ from 1948–2003 (bottom two panels). Maps on the left column are calculated using the Fexp and the Texp, i.e., $\delta\Delta pCO_{2\_var} = \Delta pCO_2(\text{Texp}) - \Delta pCO_2(\text{Fexp})$. Maps on the right column are calculated using the Ctrl and the Texp, i.e., $\delta\Delta pCO_{2\_all} = \Delta pCO_2(\text{Texp}) - \Delta pCO_2(\text{Ctrl})$.

BGD
8, 10895–10933, 2011

Simulated anthropogenic carbon uptake and data-based estimates

S. Wang et al.